

Faculty of Engineering

Faculty of Engineering - Papers

University of Wollongong

Year 2002

Order-disorder transition in
Bi_{2.1}Sr_{1.9}CaCu₂O₈ + delta single
crystals doped with Fe and Pb

K. K. Uprety* J. Horvat† X. L. Wang‡
M. Ionescu** H. K. Liu††
S. X. Dou‡‡ E. H. Brandt§

*University of Wollongong

†University of Wollongong, jhorvat@uow.edu.au

‡University of Wollongong, xiaolin@uow.edu.au

**University of Wollongong, mionescu@uow.edu.au

††University of Wollongong, hua@uow.edu.au

‡‡University of Wollongong, shi@uow.edu.au

§Max-Planck Institut fur Metallforschung, Germany

This article was originally published as: Uprety, KK, Horvat, J, Wang, XL, Ionescu, M, Liu, HK, Dou, SX, & Brandt, EH, Order-disorder transition in Bi_{2.1}Sr_{1.9}CaCu₂O₈ + delta single crystals doped with Fe and Pb, Physical review - Series B, 2002, 65, 224501 (7 pages), and may be found here. Copyright 2002 American Physical Society.

This paper is posted at Research Online.

<http://ro.uow.edu.au/engpapers/95>

Order-disorder transition in $\text{Bi}_{2.1}\text{Sr}_{1.9}\text{CaCu}_2\text{O}_{8+\delta}$ single crystals doped with Fe and Pb

K. K. Uprety, J. Horvat, X. L. Wang, M. Ionescu, H. K. Liu, and S. X. Dou

Institute for Superconducting and Electronic Materials, University of Wollongong, Wollongong, NSW 2522, Australia

E. H. Brandt

Max-Planck-Institut für Metallforschung, D-70506 Stuttgart, Germany

(Received 22 August 2001; revised manuscript received 28 December 2001; published 22 May 2002)

The magnetic field $H_{\text{dis}}(T)$ where an order-disorder transition of the vortex lattice in high- T_c superconductors occurs, is investigated by measurements of the magnetization $M(H)$ in $\text{Bi}_{2.1}\text{Sr}_{1.9}\text{CaCu}_2\text{O}_{8+\delta}$ (Bi2212) single crystals doped with iron and lead. Comparative studies are made of the temperature dependences of the field $H_{\text{peak}}(T)$, where the second peak occurs in $|M(H)|$, and the fields $H_{\text{min}}(T)$, and $H_{\text{infl}}(T)$ where a minimum and an inflection point occur at the low-field side of this peak. It is proposed that $H_{\text{dis}}(T)$ lies close to H_{infl} . In $\text{Bi}_{2.1}\text{Sr}_{1.9}\text{Ca}_{1.0}(\text{Cu}_{1-y}\text{Fe}_y)_2\text{O}_{8+\delta}$ single crystals with Fe concentration $y=0, 0.005, 0.016,$ and 0.022 , a pronounced peak in the derivative $|dM/dH|$ is observed, whose position $H_{\text{infl}}(T)$ is independent of temperature T . We relate this peak to the field $H_{\text{dis}}(T)$, which separates a weakly elastically disordered vortex lattice from a plastically disordered vortex solid. In heavily Pb-doped single Bi2212 crystals, $H_{\text{infl}}(T)$ decreases with increasing T . For the same crystals, a minimum in the normalized relaxation rate $S(H)$ is observed at H_{infl} , indicating two different flux-creep mechanisms above and below that field and two different solid vortex phases. It is argued that the negative slope of $H_{\text{dis}}(T)$ in heavily-Pb-doped Bi2212 crystals is related to the enhanced c axis conductivity caused by the Pb sitting between the CuO_2 layers and causing three-dimensional vortex lines, while in Fe-doped Bi2212 crystals the Fe ions sit on the CuO_2 planes and thus do not enhance the coupling between pancake vortices.

DOI: 10.1103/PhysRevB.65.224501

PACS number(s): 74.72.Bk, 74.60.Ge

I. INTRODUCTION

It is well established that the phase diagram of the mixed state of superconductors is characterized by various vortex phases depending on the magnetic field and temperature.¹ Due to the large anisotropy, short coherence length, and higher operating temperature of high- T_c superconductors (HTSC's), the melting lines in HTSC materials are observed well below the upper critical field H_{c2} , separating two distinct vortex phases: the vortex solid phase and vortex liquid phase.² In the vortex solid phase, the presence of quenched disorder and its interplay with thermal fluctuations appears to cause two distinctly resolved vortex solid phases: a weakly (elastically) disordered quasilattice (called the Bragg glass) and a highly (plastically) disordered solid phase (entangled solid).²⁻⁷ A steep change in the magnetization at a field H_{infl} on the low-field side of the second peak of the hysteresis loop of $\text{YBa}_2\text{Cu}_3\text{O}_{7-\delta}$, where an inflection point occurs, has been reported by Giller *et al.*⁸ The order-disorder transition of the vortex lattice has been proposed to occur near the field H_{infl} .^{2,8} Some authors assume that the order-disorder transition occurs at the second peak field H_{peak} or the field H_{min} where the magnetization has a minimum before the second peak rises.^{9,10} In this paper we shall call $H_{\text{dis}}(T)$ the field where the order-disorder transition occurs and assume that H_{dis} coincides with H_{infl} .

For less anisotropic HTSC materials such as Y123, the order-disorder transition field $H_{\text{dis}}(T)$ is observed up to the critical temperature T_c , whereas for highly anisotropic materials such as $\text{Bi}_{2.1}\text{Sr}_{1.9}\text{CaCu}_2\text{O}_{8+\delta}$ (Bi2212) single crystals, $H_{\text{dis}}(T)$ is reported up to $T=40$ K.^{1,2,4,11} Above 40 K, two vortex phases are separated by a melting line: the ordered

vortex solid and vortex liquid [or two-dimensional (2D) pancake gas] states have been reported in Bi2212 single crystals.¹ The values of $H_{\text{dis}}(T)$ are reported to change with the type of defects.^{2,9}

In this paper, we study the effects of Pb and Fe doping on the three characteristic fields $H_{\text{infl}} \approx H_{\text{dis}}(T)$, $H_{\text{peak}}(T)$, and $H_{\text{min}}(T)$ of Bi2212 single crystals. We shall show that $H_{\text{dis}}(T)$ is independent of temperature in pure and iron-doped Bi2212 single crystals, whereas in heavily-Pb-doped single crystals we find that $H_{\text{dis}}(T)$ decreases with increasing temperature. The decrease of $H_{\text{dis}}(T)$ with increasing temperature in the heavily-Pb-doped Bi2212 single crystals is the main message of this paper. We will also discuss the fact that defects positioned in the CuO_2 planes do not affect the appearance of the second peak of the hysteresis loop in Bi2212 single crystals, whereas defects introduced by decreasing the anisotropy in the same crystals strongly change the appearance of the second peak.

II. EXPERIMENTAL PROCEDURES

The lead-doped Bi2212 crystals were grown by the self-flux method, and the nominal Pb content in the lead-doped $\text{Bi}_{2-x}\text{Pb}_x\text{Sr}_2\text{CaCu}_2\text{O}_8$ crystals was $x=0.34$.¹² The dimension of the Pb-doped single crystal was $0.71 \times 1.11 \times 0.038$ mm³. The iron-doped single crystals were prepared by using the floating zone method and the nominal iron content in the $\text{Bi}_{2.1}\text{Sr}_{1.9}\text{Ca}_{1.0}(\text{Cu}_{1-y}\text{Fe}_y)_2\text{O}_8$ single crystals was $y=0, 0.005, 0.016,$ and 0.022 .¹³ The dimensions of the $y=0, 0.005, 0.016,$ and 0.022 single crystals were $1.95 \times 2.10 \times 0.116$ mm³, $1.3 \times 2.5 \times 0.15$ mm³, $1.4 \times 2.10 \times 0.026$ mm³, and $1.25 \times 1.90 \times 0.045$ mm³, respectively.

The critical temperatures of the crystals were obtained from measurements of the magnetic ac susceptibility, with the frequency and amplitude of the excitation field at 117 Hz and 0.1 Oe, respectively. Magnetic hysteresis loops and magnetic relaxation measurements were performed using an Oxford Instruments vibrating-sample magnetometer (VSM) with applied field parallel to the c axis of the crystals. In the hysteresis loop measurements, the magnetic fields were changed at a rate of 20 Oe per second, and the data were recorded at different temperatures. The hysteresis loops obtained from the magnetometer were used to calculate the critical current density J_c using the Bean relation. The equilibrium magnetization M_{eq} was obtained as $M_{eq} = (M_- + M_+)/2$, where M_- and M_+ are the branches of the hysteresis loop corresponding to decreasing and increasing applied field, respectively, and J_c was assumed to be proportional to the irreversible part $M_{irr} = |M - M_{eq}|$.

In the magnetic relaxation measurements, the crystals were first zero-field-cooled from above T_c to the desired temperature T . A magnetic field H larger than the field used in the relaxation measurements by several times the field of full penetration was applied. The field was then lowered to the measuring field, and the magnetic moment as a function of time was measured. This procedure ensured approximately a linear flux profile in the crystals. The relaxation data were recorded at different fields around the second peak of the hysteresis loop. The experimental points of the first 100 s were not included because of uncertainty in the time that passed between the establishment of the field and the measurement of the first experimental point. From our data we calculated the normalized relaxation rate $S \equiv d \ln |M_{irr}| / d \ln t$. The upper critical field H_{c2} in pure and Pb-doped single crystals was obtained from magnetization measurements by decreasing the temperature from above T_c with a constant applied field parallel to the c axis.^{14,15}

III. EXPERIMENTAL RESULTS

Figure 1 shows hysteresis loops for a heavily-Pb-doped Bi2212 single crystal. The second peaks in the heavily-Pb-doped single crystal are clearly seen at all temperatures up to T_c . This crystal had a $T_c = 69$ K. The hysteresis loops for Bi2212 single crystals with iron content $y=0$, 0.005, 0.016, and 0.022 at 24 K are shown in Fig. 2. Here, $y=0$ is a pure Bi2212 single crystal. The $y=0$, 0.005, 0.016, and 0.022 crystals had $T_c = 88.5$, 82.25, 73, and 65.5 K, respectively. The insets of Fig. 2 show hysteresis loops of these crystals at 20 K and 40 K. At or below 20 K, the second peaks are not clearly seen in Bi2212 single crystals with $y=0$, 0.005, 0.016, and 0.022, but above 20 K such peaks appear. The zero-field critical current densities at $T/T_c = 0.3$ for $y=0$, 0.005, 0.016, and 0.022 single crystals are, respectively, 1.3×10^4 A/cm², 1.7×10^4 A/cm², 2.5×10^4 A/cm², and 3.5×10^4 A/cm², whereas in heavily-Pb-doped single crystals the zero-field critical current density is 7.91×10^4 A/cm² at $T/T_c = 0.3$. Detailed results of the field dependence of the critical current density in Bi2212 crystals with $y=0$, 0.005, 0.016, and 0.022 were presented by Uprety *et al.*,¹⁶ where a strong field dependence of the critical current density was

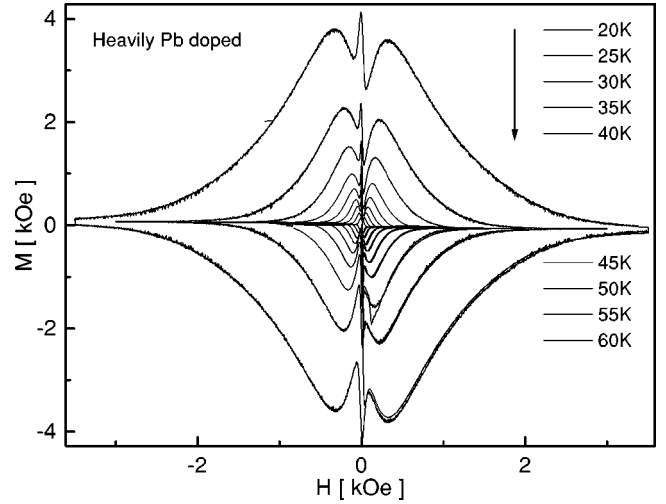


FIG. 1. The measured magnetization loops for a heavily-lead-doped Bi2212 single crystal at temperatures $T=20$ K, 25 K, 30 K, 35 K, 40 K, 45 K, 50 K, 55 K, and 60 K.

observed. However, in heavily-Pb-doped single crystals, the critical current density was weakly field dependent.¹⁷

Figures 3 and 4 show the derivative dM/dH as a function of the applied field H for pure ($y=0$) and heavily-Pb-doped single crystals. The peak in dM/dH occurs at a field $H = H_{inf}(T)$, i.e., at an inflection point of the second peak in the hysteresis loop, which we interpret as H_{dis} . The inset in Fig. 3 shows the same results for an iron-doped ($y=0.016$) single crystal. $H_{inf}(T)$ in pure and iron-doped Bi2212 single crystals is independent of temperature (Figs. 3 and 6). How-

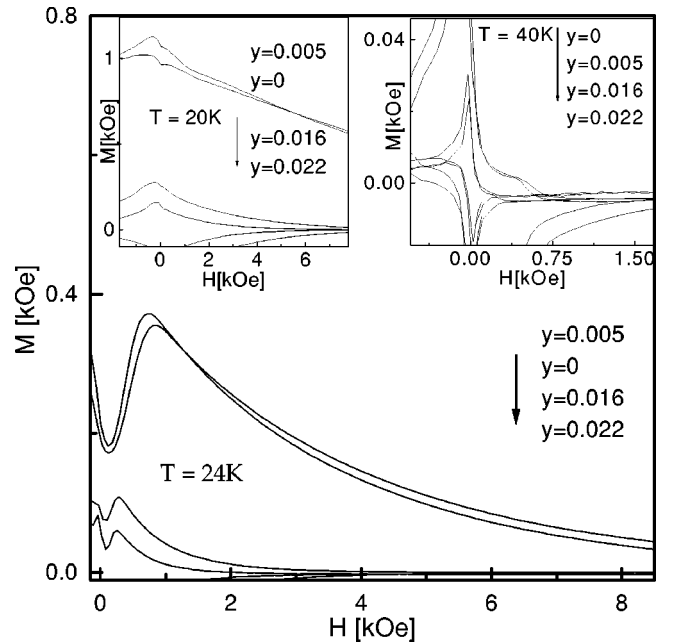


FIG. 2. The magnetic hysteresis curves for $\text{Bi}_{2.1}\text{Sr}_{1.9}\text{Ca}_{1.0}(\text{Cu}_{1-y}\text{Fe}_y)_2\text{O}_{8+\delta}$ single crystals with Fe concentration $y=0$, 0.005, 0.016, and 0.022 at $T=24$ K. The insets show hysteresis loops at $T=20$ K (right) and $T=40$ K (left) for the same materials.

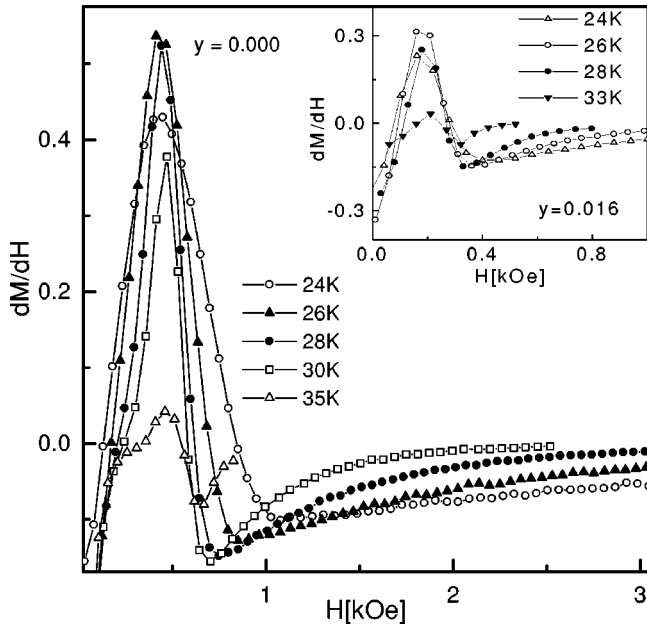


FIG. 3. The derivative dM/dH as a function of applied magnetic field H for $\text{Bi}_{2.1}\text{Sr}_{1.9}\text{Ca}_{1.0}(\text{Cu}_{1-y}\text{Fe}_y)_2\text{O}_{8+\delta}$ single crystals with zero Fe concentration ($y=0$). The inset shows dM/dH vs H for $y=0.016$.

ever, in heavily Pb doped single crystals, $H_{\text{inf}}(T)$ decreases with temperature (see Figs. 4 and 6). Figure 3 also shows an increase of $H_{\text{min}}(T)$ with T in pure and iron-doped Bi2212 single crystals. In contrast, $H_{\text{min}}(T)$ in heavily-Pb-doped Bi2212 single crystals decreases with T (see Fig. 4).

Results of magnetic relaxation measurements for Pb-doped single crystals are presented in Fig. 5. The relaxation data were recorded at various fields around the second peak

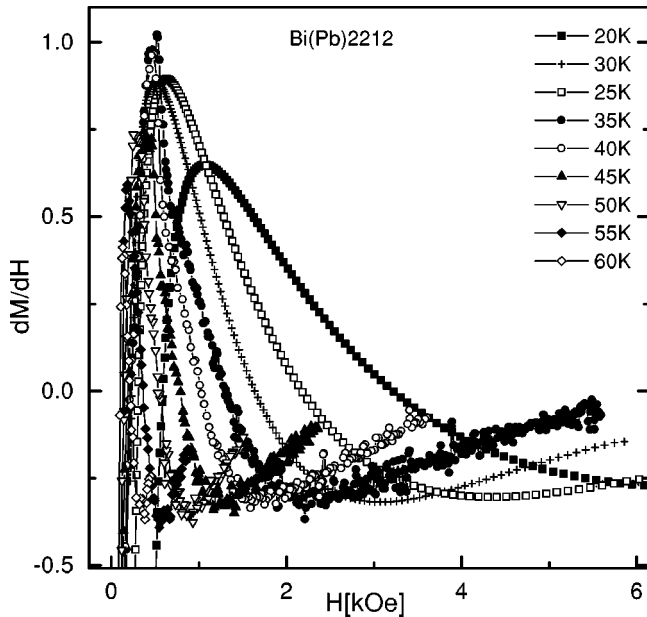


FIG. 4. The derivative dM/dH as a function of applied magnetic field H for heavily-Pb-doped single crystals.

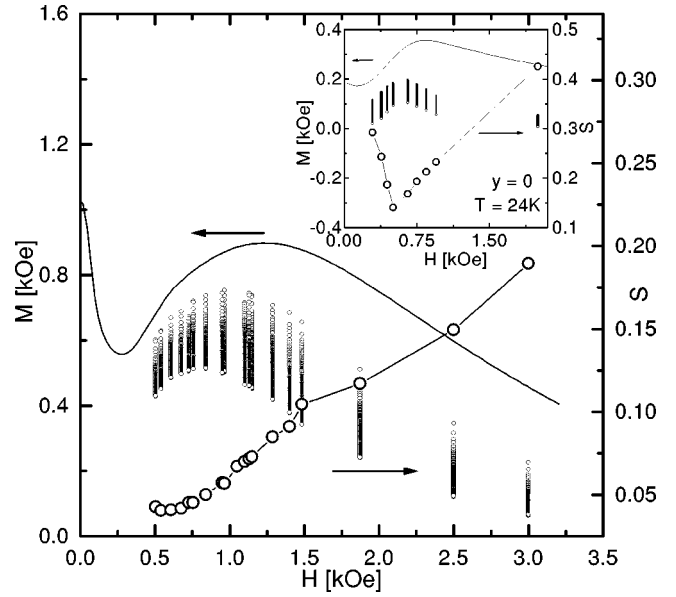


FIG. 5. The magnetization M as a function of applied field H measured at $T=35$ K for a heavily-Pb-doped single Bi2212 crystal. The small circles show the decay of the magnetization M with time t (relaxation between 100 and 3600 sec) at $T=35$ K for this crystal. The normalized relaxation rate $S = |d \ln M / d \ln t|$ is indicated by large open circles. The inset shows $M(H)$ for pure Bi2212 single crystals measured at $T=24$ K. The open and filled circles in the inset show the decay of $M(H)$ with time and the normalized relaxation rate $S(H)$ for a pure Bi2212 single crystal, respectively.

at 35 K. Figure 5 also shows the normalized relaxation rate S . The minimum in $S(H)$ occurs at H_{inf} , i.e., at the order-disorder transition field. The inset to Fig. 5 shows magnetic relaxation for a pure Bi2212 single crystal. The relaxation was recorded at various fields around the second peak at $T=24$ K. Note that the normalized relaxation rate $S(H)$ in pure Bi2212 exhibits a sharp minimum at H_{inf} .

Finally, the H - T phase diagram for the pure ($y=0$), iron-doped ($y=0.016$) and heavily-Pb-doped Bi2212 single crystals is shown in Fig. 6. A decrease of $H_{\text{max}}(T)$ with T is seen in all these crystals. Figure 6 also shows that $H_{\text{inf}}(T)$ does not depend on temperature, and $H_{\text{min}}(T)$ increases with T for pure and iron-doped single crystals. However, in the heavily-Pb-doped single crystal, $H_{\text{inf}}(T)$ and $H_{\text{min}}(T)$ both decrease with T (see Fig. 6). The upper critical field $H_{c2}(T)$ for the pure ($y=0$) and heavily-Pb-doped single crystals are also presented in Fig. 6.

IV. DISCUSSION

The pronounced second peak of the hysteresis loop $M(H)$ (peak effect) in the heavily-Pb-doped Bi2212 crystals of Fig. 1 reflects the enhanced critical current density, which depends nonmonotonically on the local magnetic field H . The second peak appears *below and above* 20 K and *persists up to* T_c . A strong peak has been reported in Y123 single crystals close to T_c .⁹ Several articles discuss the origin of the peak effect in Y123 single crystals with various types of

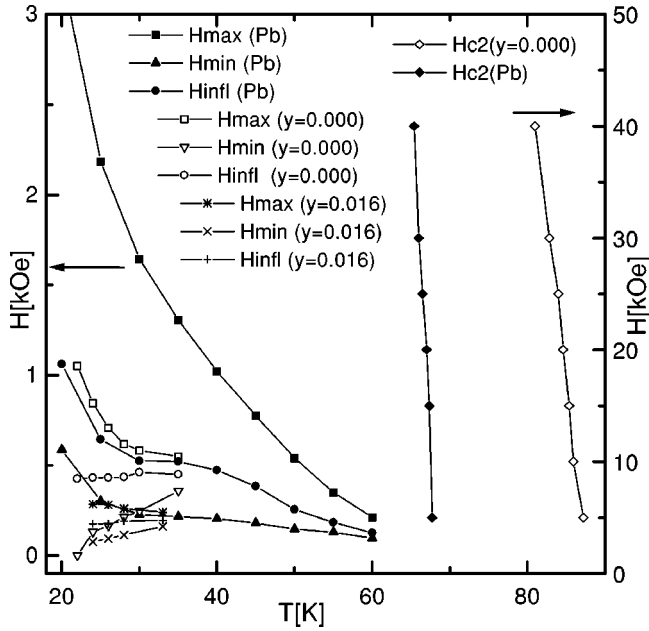


FIG. 6. The magnetic phase diagram for the $y=0, 0.016$ and Pb-doped Bi2212 single crystal. In this figure, the field of the second peak H_{peak} is denoted by H_{max} . The fields H_{min} and H_{infl} give the positions of the minimum and inflection point (or peak in the derivative dM/dH) occurring at the low-field side of the second peak. Also shown is the upper critical field $H_{c2}(T)$ for pure ($y=0$) and Pb-doped single crystals.

defects.^{2-7,9,18} In heavily-Pb-doped single crystals, Motohashi *et al.* have reported c -axis conductivity that was one order of magnitude larger than in pure Bi2212 single crystals, due to a significant reduction of anisotropy in the resistivity (ρ_c/ρ_{ab}).¹⁹ Winkler *et al.* have reported that the Josephson interlayer coupling energy increases 3.5 times with heavy Pb doping in Bi2212 single crystals.²⁰ The increased coupling energy enhances the layer coupling in the heavily-Pb-doped single crystal, which thus aligns the pancake vortices into strongly coupled stacks that behave as 3D vortex lines, similar to the vortex lines in Y123.^{17,10} We therefore believe that the strong second peak in the heavily-Pb-doped single crystals originates from the enhanced c -axis conductivity. Two-phase microstructures, i.e., lead-rich and lead-poor lamellar plates were also suggested as strong pinning centers in heavily-Pb-doped single crystals,^{21,22} which may cause a pronounced second peak.

The second peak in the hysteresis loop of pure and iron-doped Bi2212 single crystals is absent below 20 K (see Fig. 2). In pure Bi2212 single crystals below 20 K the pancake vortices are suggested to be *individually pinned*, since the Larkin correlation length along the c axis $L_c \approx (r_p/\Gamma)(J_0/J_c)^{1/2} \approx 12, \dots, 16 \text{ \AA}$ is close to the layer spacing $s = 15 \text{ \AA}$.^{23,24} Here, Γ is the anisotropy parameter, J_0 is the depairing current density at $T=0$, and $r_p \approx \xi$ (see Blatter *et al.*¹ and Refs. 24–26). These vortices are said to be in the “0D pinning region.”

An additional condition for each pancake vortex to be individually pinned is that the interplanar interaction energy

between the pancake vortices must be smaller than the pinning energy of individually pinned pancake vortices (see Blatter *et al.*¹) Below 20 K, disordered point defects can be strong pinning centers, producing a disordered vortex structure.²⁷ The absence of the second peak in the pure Bi2212 single crystals may be caused by these strong point pins. Above 20 K, the Larkin correlation length L_c grows very fast as a result of the thermal depinning.²⁴ At low fields $H \leq \Phi_0/\lambda^2$ and temperatures between 20 and 40 K, in the presence of strong point defects the vortices are in the 1D pinning region, where single vortex lines are pinned individually.²⁴ Here, λ is the penetration depth and Φ_0 is the flux quantum. In this region, the distortion of individual vortices and the proliferation of long-range topological defects in the vortex lattice are proposed as origin of the second peak.^{27,28} Above 40 K, no clear peaks are observed, see also Khaykovich *et al.*³⁰

The second peaks do not become more pronounced with iron doping in Bi2212 single crystals (see Fig. 2). As with pure single crystal, iron-doped Bi2212 single crystals have peaks between 20 K and 40 K. In the iron doped single crystals, point defects are reported to reside in the CuO_2 planes, since iron replaces Cu in the plane.²⁹ The c -axis conductivity is not improved with Fe doping in this crystal, and thus pancake coupling does not improve either. This further supports that the dimensionality of the vortices (i.e., pancake stacks or Abrikosov flux lines) plays a dominant role in the occurrence of a peak effect.

Next we discuss the effects of Pb and Fe doping on the three characteristic fields H_{min} , $H_{\text{infl}} \approx H_{\text{dis}}$, and H_{peak} of Bi2212 single crystals. It is well known that the ratio of the vortex pinning energy, the vortex elastic energy, and the thermal fluctuation energy may be used to estimate the conditions for different vortex phases to occur, namely, the vortex liquid phase, a weakly disordered quasilattice (Bragg glass), and a highly disordered solid phase (entangled or amorphous solid). The vortex liquid phase results from the competition between the elastic energy of the vortex lattice and the thermal energy kT . Similarly, the amorphous vortex solid phase may be estimated from the competition between the elastic energy and the pinning energy of the vortex lattice. The elementary pinning forces collectively interact with the elastic vortex lattice. This interaction is characterized by the size of the correlation volume $V_c \approx (4\pi/3)R_c^2 L_c$ within which the order of the vortex lattice is established and the pinning forces are correlated. Here the Larkin lengths L_c and R_c are the longitudinal and transverse sizes of the ellipsoid-shaped correlation volume.

In this paper we interpreted the inflection point H_{infl} in the magnetization curves ($|H_{\text{min}}| < |H_{\text{infl}}| < |H_{\text{max}}|$) as the field H_{dis} that separates the weakly disordered vortex lattice from the strongly disordered entangled vortex lattice. In pure Bi2212 single crystals, we observed $H_{\text{dis}} \approx 420 \text{ Oe}$ independent of temperature up to $T=40 \text{ K}$ (see Figs. 3 and 6). An order-disorder transition field $H_{\text{dis}} \approx 380 \text{ Oe}$, independent of temperature, was obtained in Hall probe measurements.^{27,30} We suggest that the pronounced peak in $|dM/dH|$ in Fig. 3,

which corresponds to the steepest change of the magnetization (inflection point) on the low-field side of the second peak, may be interpreted as H_{dis} . This definition of H_{dis} has also been used with Y123 single crystals.² The minimum observed in the normalized relaxation rate $S(H)$ of pure Bi2212 crystals in Fig. 5 also indicates two different flux creep processes in the two solid regimes: one decreasing and one increasing with increasing H . This minimum occurs at the same field as H_{infl} . Above $T=40$ K, the vortex lattice in pure Bi2212 single crystals undergoes a first order melting transition, where a negative slope of the melting line separates the vortex solid phase from the vortex liquid phase.¹

Recently, Avraham *et al.*¹¹ have observed a “melting line” below $T=40$ K in pure Bi2212 single crystals using a *shaking technique*³¹ that reduces the pinning-caused irreversibility by applying a small ac magnetic field *perpendicular* to the applied dc field. They observed a positive slope of the “melting line” at about $T=40$ K and a temperature-independent “melting line” extending to temperatures below 40 K, coinciding with the temperature-independent second magnetization peak field. The authors inferred that a first-order transition between ordered and disordered vortex phases occurs in this experiment below 40 K. However, the second peak disappears below 20 K. This might mean that the first-order transition also disappears at 20 K, implying that $T=20$ K is a critical point. But this is unlikely, because the order-disorder transition involves a change in the symmetry of the vortex structure (see also the discussion in Ref. 26). It is also possible that in Bi2212 the layers decouple at this temperature, which again can mean 0D (strong) pinning and thus may be the reason for the disappearance of the second peak. There are indeed numerous reports showing that 0D pinning sets in below 20 K in Bi2212 single crystals.^{1,24}

As with pure Bi2212 single crystals, H_{dis} in iron-doped Bi2212 single crystals was observed to be *independent* of temperature. The values of H_{dis} for single crystals with $y=0.005, 0.016, \text{ and } 0.022$ were, respectively, around 350 Oe, 185 Oe, and 170 Oe (see Figs. 3 and 6 for the $y=0.016$ crystal). However, in heavily-Pb-doped single crystals, H_{dis} was found to *decrease* with increasing temperature (see Fig. 6). In our previous paper¹⁷ we have proposed that vortices in heavily-Pb-doped single crystals are of 3D nature because of the presence of large Josephson coupling between the 2D pancake vortices in adjacent layers. The observed T dependence of $H_{\text{dis}}(T)$ in Pb-doped single crystals thus comes from its 3D behavior. Baziljevich *et al.*¹⁰ for heavily-Pb-doped Bi2212 report three regimes in the temperature dependence of the onset field H_{min} : (i) H_{min} initially decreases with T ; (ii) H_{min} then increases with T up to a maximum; (iii) H_{min} finally decreases again. These authors interpreted H_{min} as the order-disorder transition field.¹⁰

The peak field H_{peak} in all the crystals is observed to decrease with increasing temperature (see Fig. 6). The minimum field H_{min} in the pure and iron-doped Bi2212 single crystals is observed to increase with increasing temperature, whereas in heavily-Pb-doped single crystals, it is observed to decrease (see Fig. 6). The geometric and surface barriers are reported to dominate vortex pinning at low fields.^{32–34} All

our crystals were of approximately the same rectangular shape. Therefore, the effects of these barriers should not produce two opposite temperature dependences of H_{min} in pure or iron-doped Bi2212 single crystals and in heavily-Pb-doped single crystals.

According to theories, the order-disorder transition field $H_{\text{dis}}(T)$ can both increase or decrease with increasing temperature T . In Refs. 3 and 4, partly confirmed by Ref. 26, it is shown that in the single-vortex pinning region [i.e., usually at not too large H (see Ref. 26 for a detailed calculation of this regime and of the bundle pinning regime)] one finds an increasing $H_{\text{dis}}(T)$ for δl pinning (caused by spatial variations of the electron mean free path), while for δT_c pinning (caused by spatial variations of the transition temperature T_c) one has decreasing $H_{\text{dis}}(T)$. Namely, for δl pinning the temperature dependence is contained in $H_{\text{dis}}(T) \propto \xi(T)$ and for δT_c pinning one has $H_{\text{dis}}(T) \propto \xi(T)^{-3}$, where $\xi(T) \approx \xi(0)[(1+t^2)/(1-t^2)]^{1/2}$ ($t=T/T_c$ is the superconducting coherence length in the ab plane).

We have used both these functions to fit our experimental data of H_{min} , H_{infl} , and H_{peak} . Pure Bi2212 single crystals in Fig. 6 (curves $y=0$) allow us to fit $H_{\text{infl}}(T)$ by both these equations, with the choice of $H_{\text{dis}}(0)=420$ Oe. This indifference is due to the small T/T_c values, where the fitted curves show almost no temperature dependence. The more strongly T -dependent $H_{\text{min}}(T)$ and $H_{\text{peak}}(T)$ do not allow a fit by either of these formulas. A similar behavior was observed in an iron-doped Bi2212 single crystal (curves $y=0.016$ in Fig. 6) with fitted $H_{\text{dis}}(0)=180$ Oe. With the heavily-Pb-doped single crystal in Fig. 6, only the δT_c pinning formula fits our data, with $H_{\text{dis}}(0)=520$ Oe.

A complete discussion of the competing effects of T and B and of various material parameters on the various phases of the flux-line lattice with pinning is given in Ref. 26. In that work, two Lindemann criteria are applied to both thermal and pinning-caused fluctuations of 3D superconductors, defining the melting and order-disorder transitions, respectively. In this case (3D and $B=H$) the various boundaries in the h - t plane ($h=H/H_{c2}$, $t=T/T_c$) that separate the bundle-pinning from the single-vortex-pinning regime, the elastically from the plastically disordered flux-line lattices, and the solid from the melted flux-line phases depend only on two combinations of the material parameters, namely, the Ginzburg number Gi (determining the thermal fluctuations) and the combination $\xi(T)/[\Gamma L_c(T)]=\xi_c/L_c$. Here $L_c(T)$ is the Larkin pinning length (a correlation length along the flux lines) and $\xi_c(T)$ is the superconducting coherence length along the c axis (for this 3D theory to apply, $\xi_c=\xi/\Gamma$ should not be smaller than the spacing of the CuO layers). This ratio ξ_c/L_c may be written as $Dg_0(t)$, where $g_0(t)$ is a function normalized to $g_0(0)=1$ and $D=\xi_c(0)/L_c(0) \approx [j_c(0)/j_0(0)]^{1/2}$ is a material parameter, where $j_c(0)$ is the critical current density in the single-vortex-pinning regime at $T=0$ and $j_0(0)$ is the depairing current at $T=0$. If pinning by spatially varying $T_c(\mathbf{r})$ is assumed, one has $g_0(t)=(1-t^2)^{-1/6}$. Heavily-Pb-doped Bi2212 crystals have a reduced anisotropy and thus possibly may be described by this 3D theory.²⁶

V. CONCLUSIONS

Magnetization measurements have been performed in heavily-Pb-doped Bi2212 single crystals and in single crystals with iron content $y=0, 0.005, 0.016$ and 0.022 . In heavily-Pb-doped Bi2212 single crystals, strong second peaks up to the critical temperature T_c have been observed, whereas in Bi2212 crystals with $y=0, 0.005, 0.016$, and 0.022 , no peaks were observed above 40 K. We observed a decrease of the order-disorder transition field $H_{\text{dis}}(T)$ (taken from the inflection point preceding this peak) with increasing temperature in heavily-Pb-doped single crystals. This field separates two solid regimes: a weakly disordered quasi-lattice from a highly disordered solid phase. The minimum observed in the field-dependent normalized relaxation rate $S(H)$ clearly shows two different flux creep processes above and below H_{dis} , indicating two different solid phases. In Bi2212 single crystals with $y=0, 0.005, 0.016$, and 0.022 ,

H_{dis} was found to be field independent. In all crystals, the second peaks were observed to decrease with increasing temperature. The field of the minimum, $H_{\text{min}}(T)$, in crystals with $y=0, 0.005, 0.016$, and 0.022 was found to increase with increasing temperature, but in heavily-lead-doped single crystals it decreased.

ACKNOWLEDGMENTS

The authors acknowledge the support of the Australian Research Council. E.H.B. wishes to acknowledge the hospitality of the Institute for Superconducting and Electronic Materials, University of Wollongong, Australia, where part of this work was performed, and financial support from the Australian Research Council, IREX Program. We thank G. D. Gu for providing us with pure and iron-doped Bi2212 single crystals and M. J. Qin for helpful discussions.

-
- ¹G. Blatter, M. V. Feigel'man, V. B. Geshkenbein, A. I. Larkin, and V. M. Vinokur, *Rev. Mod. Phys.* **66**, 1125 (1994); D. R. Nelson and H. Sebastian Seung, *Phys. Rev. B* **39**, 9153 (1989); D. R. Nelson and V. M. Vinokur, *ibid.* **48**, 13 060 (1993); B. Khaykovich, M. Konczykowski, E. Zeldov, R. A. Doyle, D. Majer, P. H. Kes, and T. W. Li, *ibid.* **56**, R517 (1997); B. Khaykovich, E. Zeldov, D. Majer, T. W. Li, P. H. Kes, and M. Konczykowski, *Phys. Rev. Lett.* **76**, 2555 (1996); R. Wördenweber and P. H. Kes, *Cryogenics* **29**, 321 (1989).
- ²T. Nishizaki, T. Naito, S. Okayasu, A. Iwase, and N. Kobayashi, *Phys. Rev. B* **61**, 3649 (2000).
- ³V. Vinokur, B. Khaykovich, E. Zeldov, M. Konczykowski, R. A. Doyle, and P. H. Kes, *Physica C* **295**, 209 (1998).
- ⁴D. Giller, A. Shaulov, R. Abulafia, Y. Wolfus, L. Burlachkov, and Y. Yeshurun, *Phys. Rev. Lett.* **79**, 2542 (1997).
- ⁵S. Kokkaliaris, P. A. J. de Groot, S. N. Gordeev, A. A. Zhukov, R. Gagnon, and L. Taillefer, *Phys. Rev. Lett.* **82**, 5116 (1999).
- ⁶Y. Paltiel, E. Zeldov, Y. Myasoedov, M. L. Rappaport, G. Jung, S. Bhattacharya, M. J. Higgins, Z. L. Xiao, E. Y. Andrei, P. L. Gammel, and D. J. Bishop, *Phys. Rev. Lett.* **85**, 3712 (2000).
- ⁷A. E. Koshelev and V. M. Vinokur, *Phys. Rev. B* **57**, 8026 (1998).
- ⁸D. Giller, A. Shaulov, Y. Yeshurun, and J. Giapintzakis, *Phys. Rev. B* **60**, 106 (1999).
- ⁹H. K pfer, Th. Wolf, C. Lessing, A. A. Zhukov, X. Lan con, R. Meier-Hirmer, W. Schauer, and H. W hl, *Phys. Rev. B* **58**, 2886 (1998).
- ¹⁰M. Baziljevich, D. Giller, M. McElfresh, Y. Radzyner, J. Schneck, T. H. Johansen, and Y. Yeshurun, *Phys. Rev. B* **62**, 4058 (2000).
- ¹¹N. Avraham, B. Khaykovich, Y. Myasoedov, M. Rappaport, H. Shtrikman, D. E. Feldman, T. Tamegai, P. H. Kes, M. Li, M. Konczykowski, K. V. D. Beek, and E. Zeldov, *Nature (London)* **411**, 451 (2001).
- ¹²J. Horvat, X. L. Wang, and S. X. Dou, *Physica C* **324**, 211 (1999).
- ¹³G. D. Gu, G. J. Russell, and N. Koshizuka, *J. Cryst. Growth* **137**, 472 (1994).
- ¹⁴Z. Hao, J. R. Clem, M. W. McElfresh, L. Civale, A. P. Malozemoff, and F. Holtzberg, *Phys. Rev. B* **43**, 2844 (1991).
- ¹⁵U. Welp, W. K. Kwok, C. W. Crabtree, K. G. Vandervoort, and J. Z. Liu, *Phys. Rev. Lett.* **62**, 1908 (1989).
- ¹⁶K. K. Uprety, J. Horvat, X. L. Wang, G. D. Gu, H. K. Liu, and S. X. Dou, *Physica C* **341-348**, 1351 (2000).
- ¹⁷K. K. Uprety, J. Horvat, X. L. Wang, M. Ionescu, H. K. Liu, and S. X. Dou, *Semicond. Sci. Technol.* **14**, 479 (2001); K. K. Uprety, J. Horvat, X. L. Wang, M. Ionescu, H. K. Liu, and S. X. Dou, *Physica C* **341-348**, 1369 (2000).
- ¹⁸H. K pfer, A. A. Zhukov, A. Will, W. Jahn, R. Meier-Hirmer, T. Wolf, V. I. Voronkova, M. Kl ser, and K. Saito, *Phys. Rev. B* **54**, 644 (1996).
- ¹⁹T. Motohashi, Y. Nakayama, T. Fujita, K. Kitazawa, J. Shimoyama, and K. Kishio, *Phys. Rev. B* **59**, 14 080 (1999).
- ²⁰L. Winkeler, S. Sadewasser, B. Beschoten, H. Frank, F. Nouvertn  and G. G ntherrodt, *Physica C* **265**, 194 (1996).
- ²¹Z. Hiroi, I. Chong, and M. Takano, *J. Solid State Chem.* **138**, 98 (1998).
- ²²K. Itaka, H. Taoka, S. Ooi, T. Shibauchi, and T. Tamegai, *Phys. Rev. B* **60**, R9951 (1999); K. Itaka, H. Taoka, S. Ooi, T. Shibauchi, T. Tamegai, Z. Hiroi, and M. Takano, *Physica C* **341-348**, 1265 (2000).
- ²³V. F. Correa, J. A. Herbsommer, E. E. Kaul, F. de la Cruz, and G. Nieva, *Phys. Rev. B* **63**, 092502 (2001).
- ²⁴M. Niderr st, A. Suter, P. Visani, A. C. Mota, and G. Blatter, *Phys. Rev. B* **53**, 9286 (1996).
- ²⁵E. H. Brandt, *Rep. Prog. Phys.* **58**, 1495 (1995).
- ²⁶G. M. Mikitik and E. H. Brandt, *Phys. Rev. B* **64**, 184514 (2001).
- ²⁷M. F. Goffman, J. A. Herbsommer, F. de la Cruz, T. W. Li, and P. H. Kes, *Phys. Rev. B* **57**, 3663 (1998).
- ²⁸E. H. Brandt, *Phys. Rev. B* **34**, 6514 (1986).
- ²⁹B. vom Hedt, W. Lisseck, K. Westerholt, and H. Bach, *Phys. Rev. B* **49**, 9898 (1994).
- ³⁰B. Khaykovich, M. Konczykowski, E. Zeldov, R. A. Doyle, D. Majer, P. H. Kes, and T. W. Li, *Phys. Rev. B* **56**, R517 (1997).
- ³¹See also M. Willemin, C. Rossel, J. Hofer, H. Keller, A. Erb, and E. Walker, *Phys. Rev. B* **58**, R5940 (1998). A quantitative theory of this "vortex shaking" by a small transverse ac field for thin

- strips was recently given by E. H. Brandt and G. P. Mikitik (unpublished).
- ³²R. A. Doyle, S. F. W. R. Rycroft, C. D. Dewhurst, E. Zeldov, I. Tsabba, S. Reich, T. B. Doyle, T. Tamegai, and S. Ooi, *Physica C* **308**, 123 (1998).
- ³³D. T. Fuchs, E. Zeldov, M. Rappaport, T. Tamegai, S. Ooi, and H. Shtrikman, *Nature (London)* **391**, 373 (1998).
- ³⁴N. Morozov, E. Zeldov, M. Konczykowski, and R. A. Doyle, *Physica C* **291**, 113 (1997).